Journal Name

COMMUNICATION

Local visualization of catalytic activity at gas evolving electrodes using frequency-dependent scanning electrochemical microscopy

Xingxing Chen,[a,b] Artjom Maljusch,[a] Rosalba A. Rincón,[a] Alberto Battistel,[c] Aliaksandr S. Bandarenka,[a,d],* Wolfgang Schuhmann[a],*

Abstract: A new concept for the localized characterization of gas evolving electrodes based on scanning electrochemical microscopy (SECM) is suggested. It offers information about the spatial distribution of the predominant locations and dynamic characteristics of gas-bubble departure which represent the most active catalytic sites. The knowledge about gas-bubble departure is critical for the assessment and development of new electrode materials for energy applications.

One of the promising approaches to enable the increasing use of so-called renewable energy implies a wider application of electrochemical devices such as electrolyzers and fuel cells.[1,2] In general, in fuel cells dielectric properties of gaseous O_2 and H_2 phases are of less importance. In contrast, electrochemical production of H_2 and O_2 from water often leads to a stochastic, periodic or permanent blockage of the electrode surface with an insulating gas phase.[3] Thus, to further improve the performance of many types of electrolyzers, it is not sufficient to just find improved electrocatalysts. In addition, the morphology of the catalyst surface is critical; however, its role is less investigated.[4] The impact of the morphology is related to a peculiarity of electrochemical gas evolution, namely that the formation and growth of the new gas phase occurs non-evenly at specific sites across the surface, even if the catalyst loading is quasi-uniform. In an ideal situation, the density of those specific "gas evolving spots" (which are principally nucleation and growth sites for the new phase) should be maximal, and the gas bubbles should leave the surface quasi-periodically at the highest possible rate. The ability to predict and design the properties of these active spots is limited and a comprehensive characterization of surface distribution and local properties of gas evolving sites is not available. A more detailed characterization of gas evolution processes is additionally of great importance for the optimization of electrochemical Cl_2 production, which consumes approximately 1% of the electrical energy used in the world annually.[5]

Scanning electrochemical microscopy (SECM), e.g. using the sample generation-tip collection mode (SG-TC), is straightforward for acquiring detailed information about the properties and local electrocatalytic activity of gas evolving electrodes.[4,6] However, SG-TC mode SECM enables monitoring of the local electrocatalytic activity only at low current densities below gas bubble formation in order to avoid blocking of the tip electrode surface. However, this may not be sufficient to evaluate the impact of gas-bubble formation, growth and departure on the electrocatalytic properties of a catalyst.

In this work, we propose a concept for the characterization of gas evolving electrodes implementing in addition the recently developed noise mode[4a,4c,6c] of SECM together with the SG-TC mode. In a single area scan, not only information about the distribution of gas evolving sites but also the mode of the gas bubble departure at each site (e.g. periodic, quasi-periodic or stochastic) can be elucidated. It is possible to determine the characteristic frequency (v) and the amplitude (α) of the current noise generated by the periodic gas evolution and gas-bubble departure process. By multiplying these two parameters, a new parameter $\rho = v * \alpha$ is suggested which is characteristic for the periodicity of the local gas evolution process.

A four-electrode SECM system controlled by a bipotentiostat with a Pt-disk microelectrode (Ø = 25 µm)[7] as SECM tip was used. All experimental details can be found in the supporting information. RuO_2 as well as industrial O_2-evolving electrodes were used as model catalysts. All experiments were performed in air-saturated 0.1 M NaOH solution. An agar-based Ag/AgCl/3M KCl reference electrode (RE; 0.209 V vs. normal hydrogen electrode; NHE)[8] was fixed at a horizontally constant distance of 2 mm to the SECM tip and moved simultaneously. Thus, the probed distance between the tip and the RE was constant during scanning. A Pt-wire was coiled around the RE and was used as counter electrode (CE). The vertical distance between the tip and the sample surface was controlled to be 10 µm, 20 µm, or 50 µm using SECM approach curves.

Figure 1 shows a set of amplitude spectra obtained by fast Fourier transformation (FFT) of the SECM tip current over time. The tip current is due to O_2 reduction with the O_2 concentration in the gap determined by the evolved O_2 at the sample surface. The image shows O_2 evolution at a RuO_2 powder, which was pressed in the circular cavity of a recessed Au microelectrode[9] with a diameter of ~100 µm. The datasets correspond to different potentials applied at the O_2-evolving electrode. Additionally, the locally evolved and detached gas bubbles were video-monitored to further confirm the characteristic frequencies of the gas bubble detachment as obtained by FFT-spectra (see SI). Video-monitoring showed that about 58, 78, 96 and 100 bubbles were detached from the sample surface during 60 s when E_{sample} was 0.640 V, 0.650 V, 0.675 V and 0.690 V, respectively. This corresponds to $v \sim 0.97$ Hz, ~1.3 Hz, ~1.6 Hz, and ~1.67 Hz, respectively, and it is in perfect agreement with the

characteristic frequency values obtained through the FFT-spectra (Figure 1B-E). In contrast, at E_{sample} = 0.200 V, when no O_2 evolution reaction (OER) takes place at the sample, no pronounced peaks were observed in the amplitude spectrum (Figure 1A). The localized SECM tip current noise measurements at specific sites over the gas evolving surface are able to detect bubble detachment and provide information about the dynamics of this process. The appearance of characteristic frequencies in the FFT-spectra may be due to periodic changes of the resistance of a fraction of the electrolyte located between the SECM tip and the RE caused by the insulating gas phase. This change in the electrolyte resistance is described by the Bruggeman equation: $R_b=R_e(1-\varepsilon)^{-3/2}$, where R_b is the electrolyte resistance in presence of the gas phase, R_e is the electrolyte resistance without the gas phase, and ε is the gas fraction. Once the tip potential is constant any change in the electrolyte resistance results in a corresponding fluctuation of the measured tip current. Alternatively, periodic changes in the O_2 surface concentrations at the SECM tip due to local convection effects in the electrolyte and local variations of the level of supersaturation of the gas caused by the periodic bubble detachment may account for the observed tip current fluctuations.
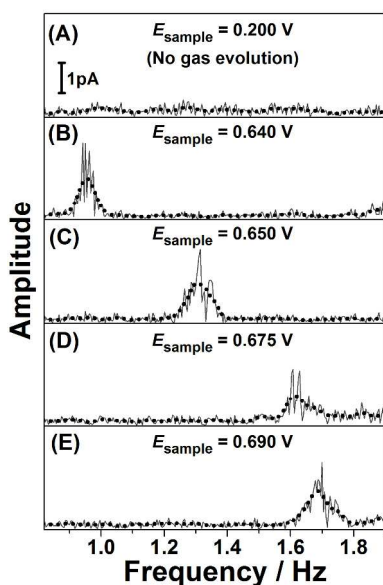
Figure 1. FFT amplitude spectra extracted from the currents recorded at the SECM tip (E_{tip} = -0.400 V, sufficiently cathodic for diffusion controlled reduction of O_2 produced at the sample surface), while the sample was polarized at potentials as indicated. Note the absence of any characteristic frequency when E_{sample} = 0.200 V at which no O_2 is evolved. The tip current was monitored with a sampling frequency of 1 kHz for 240 s. Tip-to-sample distance: 50 µm. The smoothed dotted lines is a guide to eye.

In order to use the proposed noise analysis in microscopic investigations, i.e. for evaluation of the local performance of surface sites of gas evolving electrodes, neither the characteristic frequency nor the peak maxima in the FFT amplitude spectra are alone suitable to provide information about the relative contribution of a specific spot to the overall electrode performance. For instance, if only the frequency v is selected for the visualization of the dynamic properties, the microscopic $v(x;y)$ images would not be sensitive to e.g. the distance between the SECM tip and O_2 evolving spots. Even small peaks in the FFT-spectra corresponding to positions of the SECM tip far from the site of gas bubble detachment would contribute equally to the microscopic image. If only the amplitudes α of the peaks in the FFT-spectra are selected, the dynamic properties of the revealed

O_2 evolving areas become ambiguous. Two spectra with the same amplitudes but different characteristic frequencies would contribute to the resulting microscopic images of $\alpha(x;y)$ equally. The "amplitude" refers to the variation of the tip current for the given characteristic frequency and not to the magnitude of the faradaic current. Therefore, both values, v and α should be simultaneously taken into account. Multiplication of v and α leads to the new parameter ρ =$v*\alpha$ which takes into account both criteria: the distance to the gas evolving spot and its "power" (through the amplitude) as well as the dynamic properties of the oxygen evolving site (the rate at which the bubbles leave the electrode surface). A bigger or/and faster bubble will in general refer to a higher value of ρ i.e. a more pronounced contribution of the relevant surface area to the overall catalyst activity (see SI for more information about ρ). Therefore, $\rho(x;y)$ helps in locating surface area where the change of the tip current with time is maximal. $\alpha(x;y)$ and $v(x;y)$ can be additionally evaluated (see examples in SI).

Figure 2 describes the acquisition procedure leading to $\rho(x;y)$ images. Figure 2A shows the spatial distribution of the dominant characteristic frequencies $v(x;y)$ derived from the FFT-spectra at each grid point during the area scan. As discussed above, even small peaks in the FFT-spectra related to tip positions far from the active area, contribute equally to the image. While a maximum background frequency can be selected at which no characteristic peak is observed, ambiguous values in the frequency map may be obtained in some cases. One example is also given in Figure 2A where some spots have rather high frequencies of up to ~4 Hz with small corresponding amplitudes (Figure 2B). However, one can still distinguish several truly "active" gas evolving areas (Figure 2A; e.g. at x ~ 75 µm; y ~ 75 µm) which have simultaneously significant amplitudes $\alpha(x;y)$ and characteristic frequencies $v(x;y)$ (Figure 2A and Figure 2B). Figure 2C shows the $\rho(x;y) = v(x;y) \cdot \alpha(x;y)$ image, which locates the most active gas evolving areas unequivocally at x ~ 75 µm; y ~ 75 µm by simply multiplying v and α. This is seen as a substantial improvement in comparison with previous work where stationary electrodes and only the frequency (v) were used to characterize gas evolving catalysts.[4a,4c,6c]
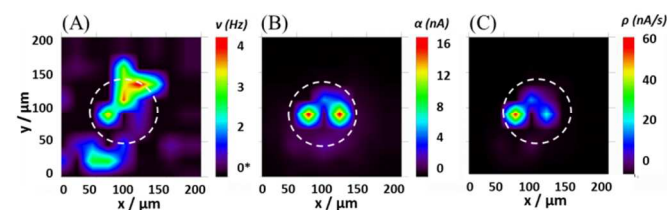
Figure 2. Spatial distributions of (A) the characteristic frequencies $v(x;y)$ available from the FFT-spectra, and (B) the corresponding amplitude map $\alpha(x;y)$. (C) shows the $\rho(x;y) = v(x;y) \cdot \alpha(x;y)$ image. White dotted lines indicate the approximate position of the circular cavity filled with RuO_2 (E_{sample} = 0.700 V, E_{tip} = -0.400 V, tip-to-sample distance: 10 µm, the tip current was monitored with a sampling frequency of 100 Hz for 60 s at each scanning grid point). The background in figure A formally starts from 0 Hz, i.e. when no characteristic frequency is detected (see SI for details).

Figure 3 represents $\rho(x;y)$ images obtained over the same sample area together with the corresponding SECM images obtained using the classic sample generation-tip collection (SG-TC) mode. In the SG-TC mode the O_2 reduction current as measured at the SECM tip is used as a measure for the activity of the local catalyst activity. However, low values of the O_2 reduction current at the tip may be not only due to a low concentration of dissolved O_2 between tip and

sample (case 1) but also to a possible blockage of the sample surface or the tip surface by gas bubbles (case 2) or the variation of the level of supersaturation due to convective effects caused by detaching gas bubbles (case 3). Therefore, the proposed visualization of local catalytic activity of gas evolving electrodes using the parameter $\rho(x;y)$ as shown in Figure 3 (top images) provides clearer information about the location of the active areas as compared to the data acquired in the classical SG-TC mode of SECM (bottom images). The parameter ρ represents a measure of a "dynamicity" of specific domains at the surface. The higher the characteristic frequency v and the higher the corresponding amplitude α in the FFT-spectra, the more significant is the relative contribution of the area to the overall catalytic activity of the surface. In the resulting $\rho(x;y)$ image, the contribution of $v(x;y)$ is mainly to reveal "dynamic" areas, while the main role of $\alpha(x;y)$ is to accurately locate the "truly active spots". The domains with the main contribution to the overall activity are located within the area filled with RuO_2 (bottom images). Moreover, the size of these active areas (top images) is smaller than those revealed by SECM in the SG-TC mode. The location of the areas with maximum $\rho(x;y)$ does not necessarily correspond to the highest SG-TC mode tip currents. Evidently, if the SECM tip is positioned exactly over a gas-evolving active area, the small gap between tip and sample is immediately filled with gaseous O_2 thus reducing the electrolyte contact between the SECM tip and the RE. This may also lead to decreased oxygen-reduction currents at the SECM tip in the SG-TC mode of SECM (more explanation with a schematic drawing is presented in SI). Additionally, mainly convective phenomena caused by the bubble departure or topographic restrictions may cause asymmetries in the SG-TC SECM images (Figure 3, bottom line). In contrast, the frequency of gas-bubble departure and the amplitude in the FFT spectra are maximal in this case.
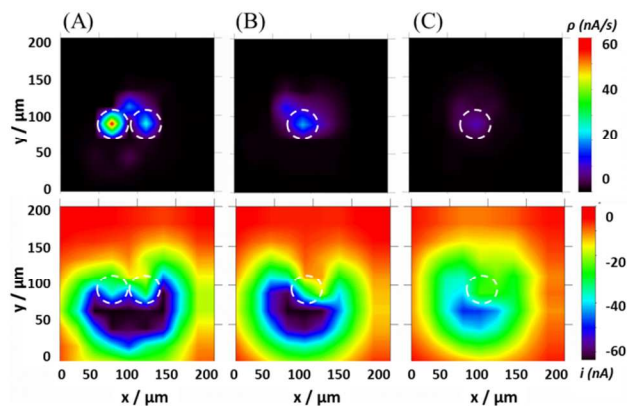
Figure 3. (A-C, top line) successive amplitude-by-frequency, $\rho(x;y)$, images (left to right, recorded every 80 min) and (A-C, bottom line) corresponding SECM images recorded in SG-TC mode taken simultaneously over the same RuO_2 surface. White dashed lines indicate the approximate position of the active areas (E_{sample} = 0.700 V, E_{tip} = -0.400 V, tip-to-sample distance: 10 µm, the tip current was monitored with a sampling frequency of 100 Hz for 60 s at each scanning grid point). Pure RuO_2 is known to be unstable under the selected experimental conditions; thus, the figures reveal deactivation of the catalyst with time from A to C.

Figure 4 shows SECM images of the surface of a commercial dimensionally stable anode (DSA) using the SG-TC mode (Figure 4A) and the noise mode with the corresponding amplitude-by-frequency, $\rho(x;y)$ images (Figure 4B). The SG-TC mode image identifies three interesting domains designated as 1, 2 and 3 in the figure. The rela-

tively small circular domains 1 and 2 appear as "non-active" exhibiting very low O_2 reduction currents at the tip which are even below the background current defined by dissolved O_2. In contrast, the extended domain 3 in Figure 4A appears as "active", with a measured tip current which is significantly more negative than the background current. The corresponding $\rho(x;y)$ image (Figure 4B) reveals that domain 1 is an active area demonstrating that the dynamics of the gas bubble departure is efficiently removing dissolved O_2. Domain 2 also appears as active (Figure 4B) but its contribution is significantly lower than that of domain 1. This difference originates from the fact that the characteristic frequency and the corresponding amplitude are lower for domain 2 (see SI). Interestingly, domain 3 does not show any significant dynamicity. We hypothesize that it is permanently blocked by gas bubble(s).
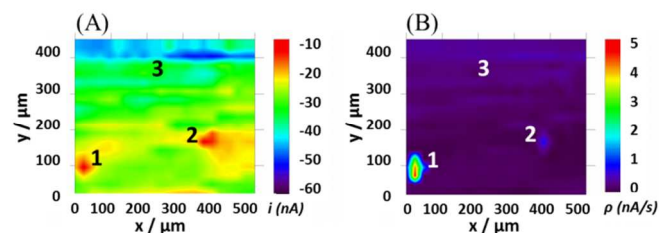
Figure 4. Characterization of an industrial DSA anode under O_2 evolution conditions (E_s = 0.700 V, E_{tip} = -0.400 V, tip-to-sample distance: 20 µm, the tip current was monitored with a sampling frequency of 100 Hz for 60 s at each scanning grid point). (A) SG-TC mode image and (B) corresponding amplitude-by-frequency, $\rho(x;y)$, image of the same electrode area.

In summary, we have demonstrated a novel concept for a detailed SECM characterization of gas evolving electrodes based on the combination of both the noise and SG-TC modes of SECM. An objective mean of how to assess the dynamic properties of gas evolving areas on catalyst surfaces is provided allowing distinguishing areas at the surface of gas evolving electrodes, which primarily contribute to the overall electrocatalytic activity in form of gas bubble production. Moreover, this approach can be implemented for investigating industrial gas evolving electrodes. Further elaboration of this method, including improved temporal resolution for less stable electrocatalysts, will provide a research tool for gaining improved understanding of how to design and optimize the electrode surface for electrochemical gas production processes.

Notes and references

[a] Center for Electrochemical Sciences (CES), Ruhr-Universität Bochum, Universitätsstr. 150, D-44780 Bochum, Germany; E-mail: aliaksandr.bandarenka@rub.de, wolfgang.schuhmann@rub.de

[b] School of Chemical Engineering, University of Science and Technology Liaoning, Qianshan Road 185, 114051 Anshan, China

[c] Semiconductor & Energy Conversion – Center for Electrochemical Sciences (CES); Ruhr Universität-Bochum, Universitätsstr. 150, D-44780 Bochum, Germany

1   (a) H.A. Gasteiger and N.M. Markovic, *Science*, 2009, **324**, 48; (b) A. Rabis, P. Rodriguez, and T.J. Schmidt, *ACS Catal*., 2012, **2**, 864; (c) I.E.L. Stephens, A.S. Bondarenko, U. Grønbjerg, J. Rossmeisl, and I. Chorkendorff, *Energy & Environ. Sci.* 2012, **5**, 6744; (d) M. Carmo, D.L. Fritz, J. Mergel, and D. Stolten, *Int. J. Hydrogen Energy*, 2013, **38**, 4901; (e)   N. Armaroli and V. Balzani, *ChemSusChem*, 2011, **4**, 21.

2   S. Chu and A. Majumdar, *Nature*, 2012, **488**, 294.

3   M. Wang, Z. Wang, X. Gong, and Z. Guo, *Renew. Sust. Energ. Rev.*, 2014, **29**, 573.

4   (a) A.R. Zeradjanin, A. A. Topalov, Q. van Overmeere, S. Cherevko, X.X. Chen, E. Ventosa, W. Schuhmann, and K.J.J. Mayrhofer, *RSC Adv.* 2014, **4**, 9579; (b) L.A. Naslund, C.M. Sanchez-Sanchez, A.S. Ingason, J. Backstrom, E. herrero, J. Rosen, and S. Holmin, *J. Phys. Chem. C*, 2013, **117**, 6126; (c) A.R. Zeradjanin, E. Ventosa, A.S. Bondarenko, and W. Schuhmann, *ChemSusChem*, 2012, **5**, 1905;

5   M. Grotheer, R. Alkire, and R. Varjian, *Electrochem. Soc. Interface*, 2006, **15**, 52.

6   (a) A. Maljusch, E. Ventosa, R.A. Rincon, A.S. Bandarenka, and W. Schuhmann, *Electrochem. Commun*., 2014, 38, 142; (b) H.S. Park, K.C. Leonard, and A.J. Bard, *J. Phys. Chem. C*, 2013, **117**, 12093; (c) A.R. Zeradjanin, T. Schilling, S. Seisel, M. Bron, and W. Schuhmann, *Anal. Chem*., 2011, **83**, 7645; (d) S. Schmachtel, S.E. Pust, K. Kontturi, O. Forsen, and G. Wittstock, *J. Appl. Electrochem.*, 2010, **40**, 581; (e) G.A. Snook, N.W. Duffy, and A.G. Pandolfo, *J. Electrochem. Soc.*, 2008, **155**, A262; (f) A. Minguzzi, M.A. Alpuche-Aviles, J.R. Lopez, S. Rondinini, and A.J. Bard, *Anal. Chem.*, 2008, **80**, 4055.

7   (a) F.R.F. Fan and C. Demaille, in: A.J. Bard and M.V. Mirkin (Eds.), Scanning Electrochemical Microscopy, Marcel Dekker: New York, 2001; (b) M. Kranz, H. Ludwig, E. Gaub, and W. Schuhmann, *Adv. Mater.*, 1995, **7**, 568.

8   A.W. Hassel, K. Fushimi, and M. Seo, *Electrochem. Commun*. 1999, **1**, 180.

9   (a) B. Zhang, Y. Zhang, and H.S. White*, Anal. Chem.* 2004, **76**, 6229; (b) B. Zhang, J. Galusha, P.G. Shiozawa, G. Wang, A.J. Bergren, R.M. Jones, R.J. White, E.N. Ervin, C.C. Cauley, and H.S. White*, Anal. Chem.* 2007, **79**, 4778.

207x68mm (150 x 150 DPI)